

Wax-bonding 3D microfluidic chips†

Xiuqing Gong,^a Xin Yi,^a Kang Xiao,^b Shunbo Li,^a Rimantas Kodzius,^c Jianhua Qin^{*d} and Weijia Wen^{*ac}

Received 29th March 2010, Accepted 9th June 2010

DOI: 10.1039/c004744a

We report a simple, low-cost and detachable microfluidic chip incorporating easily accessible paper, glass slides or other polymer films as the chip materials along with adhesive wax as the recycling bonding material. We use a laser to cut through the paper or film to form patterns and then sandwich the paper and film between glass sheets or polymer membranes. The hot-melt adhesive wax can realize bridge bonding between various materials, for example, paper, polymethylmethacrylate (PMMA) film, glass sheets, or metal plate. The bonding process is reversible and the wax is reusable through a melting and cooling process. With this process, a three-dimensional (3D) microfluidic chip is achievable by evacuating and venting the chip in a hot-water bath. To study the biocompatibility and applicability of the wax-based microfluidic chip, we tested the PCR compatibility with the chip materials first. Then we applied the wax-paper based microfluidic chip to HeLa cell electroporation (EP). Subsequently, a prototype of a 5-layer 3D chip was fabricated by multilayer wax bonding. To check the sealing ability and the durability of the chip, green fluorescence protein (GFP) recombinant *Escherichia coli* (*E. coli*) bacteria were cultured, with which the chemotaxis of *E. coli* was studied in order to determine the influence of antibiotic ciprofloxacin concentration on the *E. coli* migration.

Introduction

Development in microfluidics has spurred growing interest in low-cost, straightforward and rapid prototyping of microfluidic devices. One of the most popular methods is soft-lithography which uses a soft polymer such as poly(dimethylsiloxane) (PDMS) to imprint and transfer the structure on a well patterned photoresist.^{1–5} PDMS, compared with other materials, has advantageous properties including typically low surface interfacial free energy, which enables it to conform to the surface of a master; an elastic characteristic, which allows it to be easily removed; and optical transparency, which improves transmission of UV and visible light. Although PDMS based microfluidic devices have been widely employed due to their ease of fabrication, there remain some shortcomings. For example, PDMS absorbs small, hydrophobic molecules and the water evaporates through the PDMS pores, which may affect microfluidic chip efficiency when it compromises the cell culture media.^{6–9} Another disadvantage of PDMS is the difficulty of complex 3D structures by multilayer bonding; accompanying this usually requires a silane coupling agent to treat the PDMS surface, as well as laborious layer-by-layer bonding.^{10,11} Besides, the poor adhesion between metal and PDMS makes direct patterning of a conductive metal layer on the PDMS surface problematic.¹² An

alternative method for rapid and inexpensive chip bonding is called “print-to-cast”,^{13–21} for example the thermal pattern of wax. Methods in this area are majorly paper-based microfluidic chips. Take the thermal printer-based chip fabrication method for example.¹⁴ The process, utilizing a wax printer to pattern hydrophobic wax walls directly in the hydrophilic paper, is less time consuming and low cost. Moreover, the hydrophobic pattern enables biological fluid transport by means of capillary action in the micron-sized-porous cellulose. Nevertheless, because the fluid cannot form continuous flow in the paper, this application meets many limitations. The droplet cannot be formed by the paper chip; the liquid transport velocity depends on the passive capillary action and cannot be actively changed; the cellulose fiber has absorption on many molecules; the chip is usually an open system and easily effected by the ambient environment; it is difficult to pattern electrodes in a cellulose network. In this circumstance, the paper chip is applied mostly to develop simple, easy-to-fabricate, and inexpensive point-of-care tools for fast diagnostic applications.

To complement the new functionalities and applications being developed in the microfluidic field, especially the all-in-one system that is envisaged, a highly functionalized, ease-to-fabricate and low-cost microfluidic chip is required. In fact, opportunities abound, as there are a variety of inexpensive materials that can be utilized besides PDMS,^{22–26} which are easily and inexpensively machinable by both mechanical cutting²⁷ or laser devices.^{28–30} Such materials contain thin films or paper sheets which are easily accessible in daily life, like A4 paper (thickness: approximately 100 μm), transparent overhead-projector film, and PMMA plates, though the problem of how to bond them together quickly and effectively remains. The chip bonding techniques reported include adhesive glue bonding, solvent evaporation bonding, localized welding, or surface treatment and modification *etc.*³¹ The glue and solvent bonding is restricted to specific materials; thermal fusion and welding bonding can not

^aDepartment of Physics, The Hong Kong University of Science and Technology, Clear Water Bay, Kowloon, Hong Kong. E-mail: phwen@ust.hk

^bDepartment of Biology, The Hong Kong University of Science and Technology, Clear Water Bay, Kowloon, Hong Kong

^cKAUST-HKUST Micro/Nanofluidic Joint Laboratory, The Hong Kong University of Science and Technology, Clear Water Bay, Kowloon, Hong Kong

^dDalian Institute of Chemical Physics, Chinese Academy of Sciences, 457, Zhongshan Road, 11603, China. E-mail: jhqin@dicp.ac.cn

† Electronic supplementary information (ESI) available: PCR biocompatibility with materials. See DOI: 10.1039/c004744a

be applied to thin film (if $<100\ \mu\text{m}$); surface modification usually requires complex chemical treatment. Recently, double-sided pressure sensitive adhesive (PSA) tape was introduced to chip bonding.^{15,31} Although this method is very cheap and convenient, the chemical composition of the adhesive is usually too complex for biological samples, for example the bonding strength is sensitive to environmental humidity and temperature, the bridge bonding between different materials (*e.g.* between glass and PMMA) is difficult.

In this study, we propose a hot melt bonding method, including the bonding material and technology. With it, different materials can be reversibly bonded together. One-step bonding of multiple layers together into 3D structure can also be realized. The bonding material is a simple hydrocarbon-alkyl-based adhesive wax which can adhere to the material surface when melting because of the low interfacial energy like PDMS. After cooling, adhesion is maintained without incident under exposure both to aqueous and acid solvent. The wax bonding, indeed, offers excellent bonding strength, and was designed to adhere to a wide range of substrates. In the semiconductor field, wax bonding is normally used to hold wafer in place during slicing, dicing, polishing and lapping process.³² In the present study, we apply the wax bonding technology to microfluidic chip fabrication. We first evaluate the biocompatibility of materials employed in the chip fabrication, including PMMA, PC, paper and wax. To do so, we use the polymerase chain reaction (PCR), one of the most frequently used enzymatic reactions in microfluidics, as a model in an investigation of the PCR-inhibitory effect. To fabricate chip, we fill selected paper with melt wax and sandwich it between different materials to form a wax-paper-based chip. Electrodes could be integrated into the chip for the purpose of HeLa cell electroporation. A prototype of 3D structure could also be fabricated by a single step. A bacterial culture is utilized to test its sealing ability and durability. The 3D chip demonstrates utility with a drug screening system designed to test the influence of drug concentration on bacterial chemotaxis.

Methods

Laser cutting for different materials

We use a CO₂ laser (Versa Laser System, model VR3.50, Universal Laser Systems, Ltd.) to cut through thin-layer materials in a continuous mode. The focal spot size is about $100\ \mu\text{m}$ in width. The laser power varies from 5 W to 20 W and with the cutting velocity $0.76\ \text{mm s}^{-1}$. For example, to cut through A4 paper, 5 watt power easily burns the paper and produces exact and uniform grooves along the entire length of the worked surface. The laser has been put to a wide range of uses in the field of organic soft matter. Such matter vaporizes to gaseous compounds upon laser cutting, and so a very clean cut can be performed.^{33,34} Intricate designs can be formed at high cutting velocity, without any stress or deformation of the organic film at 20 watt power. The channel dimension not only can be adjusted by varying the laser power of source, the scan speed, and the focus point, but also depends on the composition and thickness of the cutting materials. For a $100\ \mu\text{m}$ -thick A4 wood paper sheet, the smallest size obtainable is around $50\ \mu\text{m}$ in width, whereas for $90\ \mu\text{m}$ -thick transparent film, about $100\ \mu\text{m}$. For the purpose of the present study, the thin film materials employed included A4 wood paper acquired from Fuji Xerox (Japan), transparent film (polypropene, about $90\ \mu\text{m}$ in thickness as measured) obtained from 3M Company (USA), PMMA (1 mm in thickness) and polycarbonate (PC, $500\ \mu\text{m}$ in thickness) membrane purchased from Techplast coated Product, Inc. (USA).

Wax bonding

The materials used in the preparation of microfluidic chips, shown in Fig. 1a, are easily accessible and inexpensive. For the paper-based chip, we first use a scalpel or laser to cut a channel in the paper, after which we let the paper absorb the hot melt adhesive wax (purchased from Nikka Seiko [Skywax Series,

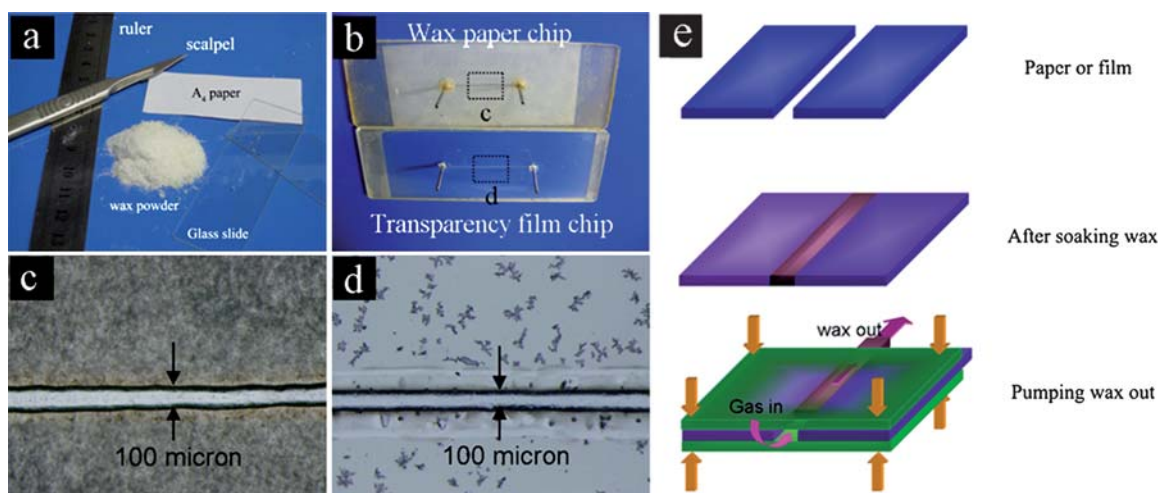


Fig. 1 (a) Materials required for a simple 2D chip. A ruler and scalpel were used to align and cut the channel in the paper. Wax powder was used to fill the paper and bond it with the glass slide, (b) prototype of a paper-based chip (c) and a film-based chip (d). (c) and (d) are magnified pictures corresponding to the selected area in (b), (e) flow chart of chip bonding. After laser cutting, the paper or film absorbed wax at the wax's melting point. After cooling, the film or paper was sandwiched between two glass slides and immersed in a hot-water bath. The gas was introduced from the inlet to the outlet through which the wax in the channel was pushed.

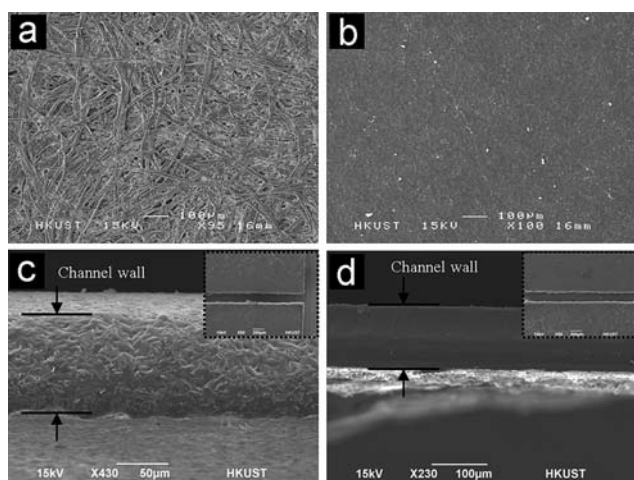


Fig. 2 (a) Surface morphology of A4 wood paper before absorbing wax, (b) after absorbing wax, (c) channel wall of wax-filled paper, (d) channel wall of transparent film. The inset pictures are the corresponding wax paper and transparent film channels.

Japan]) for 10 min at the melting point 60 °C. After cooling down, the wax paper is sandwiched between two glass slides in which inlet and outlet holes have been drilled (Fig. 1b). These three layers are pressed together by four clamps at four corners and the bonding process is finished in a hot-water bath (70 °C), using a syringe filled with gas to manually control the gas pressure, the pressure slowly pushes out the wax (Fig. 1e). After rinsing it under cool water, the wax between the different layers solidifies, enabling their adhesion. The thin layer of wax (about 1-2 μm as determined by stepper scan) reserved in the cover or lower layer could be flushed off by flowing ethanol to wash the channel. The resultant wax-paper chip has an opaque appearance owing to the non-transparency of the paper. To make a transparent chip, we substitute the transparent film for paper (Fig. 1b). Fig. 1c and d are the top views of the channels cut in the wax paper and transparent film. It can be seen that the channel edge made of the transparent film (Fig. 1d) is sharper than in the wax paper (Fig. 1c). That is because the surface of the paper wall is rougher and more porous. To make a comparison, we scanned the surface morphology of the paper and film using SEM. Fig. 2a shows the surface structure of the paper, which is interconnected by millimetre-sized cellulose. Fig. 2b shows the paper surface after having absorbed wax and being compressed by the glass slide. As is apparent, the surface became smooth, adhering tightly to the glass slide. Fig. 2c and d are the surface morphologies of the paper and film channel wall. Clearly, the channel wall cut into the wax paper is rougher than that in the transparent film, which corresponds to Fig. 1c and d. The bonding strength of wax-paper chip is defined by the highest air pressure that can be sustained in the chip. (Table. S1.)† The bonding strength for wax-paper between glass is about 340 kPa, and between PMMA 370 kPa.

3D microfluidic chip

Wax bonding can also be applied to the fabrication of complex 3D structures in different materials. The process to fabricate

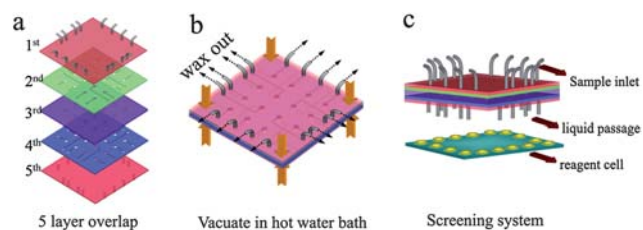


Fig. 3 (a) Five layers were overlapped and aligned. All of the layers were wetted by melt wax before being overlapped. (b) Layers were pressed together by four clamps at four corners (yellow arrows). (c) Structure of bacterial screening system comprised of an upper screening chamber and a lower reagent cell. The liquid passage was a glass capillary which allowed the movement of liquid by capillary action.

a 3D microfluidic chip is shown in Fig. 3. The chip is composed of five layers of which the 1st and 5th layer are 1 mm-thick pyrex glass slides, the 2nd and 4th layer are 1 mm-thick PMMA, and the 3rd layer is 500 μm -thick PC (Fig. 3a). Inlet and outlet holes have been drilled in the glass slides which are connected by steel tubes (sample inlet, 1 mm in dimension) and glass capillaries (liquid passage, 1 mm in dimension). The 3rd layer is a 4×4 array for the screening chamber. The width of the chamber is 2 mm. On both sides of the 3rd layer are the channel layers (2nd and 4th), which guide the flow of liquids and lead them to the screening chambers. The channel is 200 μm in width. They all are formed by laser-cutting through the thin materials with 20 watt power. Preparatory to the assembly of the layers, the PMMA and PC layers are immersed into melt wax. After taking them out, the five layers are overlapped and well aligned before being placed in a hot-water (red ink dyed) bath (70 °C) in a vacuum oven (SHEL LAB, USA). Four clamps were used to hold all of the layers together at their four corners (yellow label in Fig. 3b). After vacuumating the chamber, the melt wax will be driven out from the inlet and outlet of the chip, floating to the top layer of water bath because the melting wax has lower density than water. Repeat venting and evacuating several times to make sure all the channels are filled with water (judge by the indicator of red color). Then, take the chip out and flush it with cool water. A reagent cell (Fig. 3c) was also fabricated by laser cutting in the PMMA board. The width of the cell is 1.5 mm. The structure of the 3D screening system is shown in Fig. 3c. The wax-paper can also be utilized to bond the 3D chip with the same process. Fig. S2† shows how 3 sheets of wax-paper are bonded together by two glass slides.

Materials investigated

The following materials were first tested for enzymatic compatibility: PMMA, PC, pyrex glass, A4 printing paper, wax and paper impregnated with the wax. The materials were manually broken into small fragments and a sample of size $>5 \text{ mm}^2$ to each PCR reaction tube was added (see the supplementary information†).

Material enzymatic biocompatibility

A large number of materials, including silicon, glass, various plastics and others, are currently used in microfluidics chip

production. When these materials come in contact with biomolecular reaction components, adsorption and inhibition of biomolecules arise as problems to be avoided.^{35,36} In this issue, we first assessed material biocompatibility by testing the PCR-inhibitory of chip materials. Biocompatibility of materials can be measured on a DNA, RNA, protein (enzymatic) or cellular level. PCR reaction contains both DNA and enzyme (polymerase). Therefore we chose PCR for material biocompatibility testing. A PCR mix incubated with materials but without BSA provided clues as to which materials are PCR-inhibitory. Most bio-friendly materials exhibit similar signals regardless of the inclusion or not of BSA in the PCR mix: these are PMMA, PC and pyrex glass and wax. The signal is comparable to the no additive control's (Fig. S1†). In this study, no signal was obtained in the PCR mix incubated with paper despite BSA inclusion. Interestingly, a signal was obtained in PCR including paper impregnated with the wax with the addition of BSA. The signal strength was similar to the PCR with included wax material. Although the fluorescent signal is not very strong, these results show that wax impregnated paper behaves differently than pure paper by possibly compromising the absorption of DNA and protein by paper. Moreover, there are other different types of wax, as it is inert, we do not expect many waxes to interact with PCR components. For example, wax is even until now used to cover PCR mixtures and avoid evaporation. As a result, it is possible to use wax to realize some biological process which cannot be fulfilled by paper, avoiding PCR-inhibition and should be biocompatible with enzymes. In Fig. S1,† the bright signal at the loading well originates probably from the remaining paper fibres which strongly absorb the UV light and give bright fluorescence.

Wax paper chip for electroporation

Electroporation (EP) has been used as a powerful cell transfection method which is to deliver membrane-impermeable macromolecules into cells.^{37,38} The advantage of on-chip electroporation is a small quantity of samples and an uniform electric field in these narrow regions, which helps to enhance both cell viability and EP efficiency with few side effects that are known to exist in the conventional devices.^{39–43} Wax bonding provides an effective way of metal bonding and electrode imbedding. To test the uniformity of the electric field, we sputtered 10 nm-thick gold onto glass slides as the cover and lower layer, and sandwiched wax paper between them to bond them together.

The chip bonding process is shown in Fig. 4a. Both the channel width and depth were 100 μm . The planar electrode area is 100 μm in width and 2 cm in length. We performed an experiment of red dye intake into HeLa cells for various electric fields generated in the channel. HeLa cells obtained from the American Type Culture Collection (ATCC, Manassas, VA) are suspended in the poration medium containing dextran, rhodamine B isothiocyanate, 70S (R-9379), purchased from Sigma, and then filled into one channel. The density of the cells in the poration medium is about 10^5 cells ml^{-1} . The volume of the mixture in the electrode area is about 0.2 μl . The sample volume is controlled by syringe pump. We blow N_2 gas into another channel to push the sample. The electrodes are connected to a radio-frequency (RF)-oscillating electric pulse generator (Bio-Rad Labs). Two trains of electric pulses are applied to the cell/dye mixture suspension at 10 s intervals. The waveforms of the output electric pulses are monitored using a digital storage oscilloscope (Tektronix 2221A). There are 10 pulses in each train. The frequency is 30 kHz, duration time of each pulse is 5 ms and the interval between each pulse is 100 ms. After applying different voltages, the cells under bright and fluorescent field are counted. The viability as well as EP efficiency is listed as shown in Fig. 4b. Applying 30 volt to the electrodes could get better viability as well as EP efficiency than 20 volt and 40 volt. The mean viability is $84.25 \pm 8.63\%$, accompanying with the EP efficiency $52.91 \pm 2.68\%$. The result first indicates the wax can be utilized to bond metal electrodes with chip together. Second, there is no liquid leakage appearing in the channel even after repeated usage. This means that the wax has good sealing ability which can hold different materials together. Third, we do not see the cell trapping phenomenon in the chip under microscopy which suggests that the wax has no absorption on the cells during the EP process. The wax-bonded electrodes can also be applied to other electro-dynamic processes, for example electrophoresis, or on chip electro-detection.

3D chip for bacterial culture and screening

To test the durability of the wax bonded 3D microfluidic chip (Fig. 3), we apply it to the culture and screen of GFP (green fluorescence protein) recombinant *E. coli* bacterial. Fig. 5a is the top view of the transparent chip. Fig. 5b shows the flow line of liquid in the 3D chip as we infuse red dye solution to the chip. The chemotactically wide type *E. coli* strain is a motile strain with

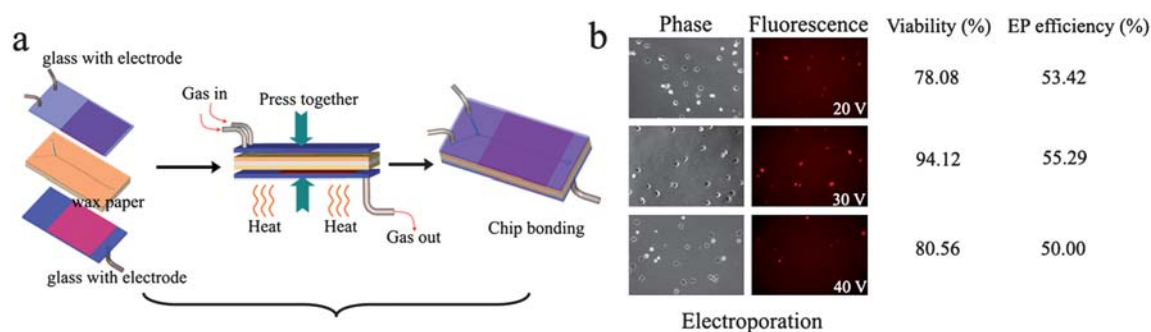


Fig. 4 (a) The flow chart to show the fabricating process of a wax-paper-based microfluidic device with imbedded electrodes. (b) The images of cells under bright field and fluorescent field. The cell viability and the EP efficiency are also presented.

RP437 transformed with a high copy plasmid expressing ampicillin resistance and GFP expression. To culture the *E. coli*, we first infuse the standard growth medium L-Broth to the sixteen screening chambers from the sample inlet (Fig. 3c), one liter of medium containing 10 g of tryptone, 5 g of yeast extract, 10 g of sodium chloride, and 2 ml of ampicillin solution (100 mg ml^{-1}). One *E. coli* bacterial colony on the agar plate is transferred to the tube with 3 ml L-Broth and $10 \mu\text{M}$ ampicillin. The tube is incubated and shaken at $30 \text{ }^\circ\text{C}$ for 6 h. One droplet of the bacterial broth is added to the 16 reagent cells. Then, the liquid passage of the screening device is inserted into the reagent cell. The *E. coli* bacteria migrate through the glass capillary to the screening chamber full of food resources, where they proliferate and express strong green fluorescence. The GFP labeled bacteria are imaged by an inverted fluorescence microscope (Axiovert 200M, Zeiss) equipped with a cooled CCD camera (Diagnostic Instruments). The full-range-picture is taken by a Canon camera (EOS 5D, Mark II) equipped with a macro lens (MP-E, 1–5 \times). The image data acquired from the CCD camera are further processed and analyzed by MetaMorph (Universal Imaging Corp.). Quantitative analysis is carried out with the help of Excel (Microsoft), and refined images are done by Confocal Assistant v4.0 (Bio-Rad) and Adobe Photoshop. The motion of cells upwards from the reagent cells to the food-enriched screen chambers occurs as all the channels were full of fluorescence which interacts through chemotactic signaling in the bacterial system.^{44,45} Eventually, at about 15 days all of the chambers are full of GFP fluorescence. The fluorescent images and the fluorescence intensity measurement (Fig. 5c, A, B, C, and D) indicate that the bacteria undergo a uniform rate of proliferation throughout the chambers. The *E. coli* bacteria recover motility

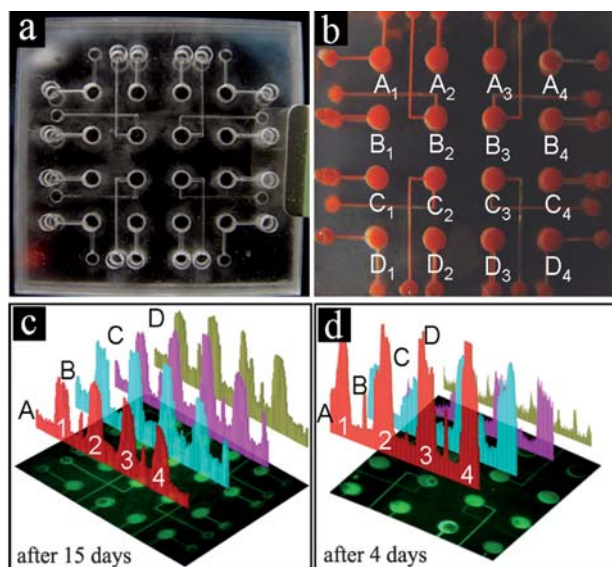


Fig. 5 (a) Top view of 5-layer 3D structure, (b) Red dye solution was infused to indicate screening chambers, (c) GFP recombinant *E. coli* bacteria were cultured in screening chambers showing green fluorescence protein. The peaks appearing in rows A, B, C, and D labeled by digits 1, 2, 3, and 4 show the intensity of fluorescence corresponding to the screening chamber beneath them, (d) the chemotaxis phenomenon of *E. coli* bacteria responding to the antibiotic concentration.

after we detach the chip and culture them again in the tube. The result proves that the 3D microfluidic chip could endure long time bacterial culture without liquid leakage even after 15 days incubation, and the screening system is compatible with the bacterial culture. To demonstrate the drug screen performance, we add different concentrations of antibiotic solution to the reagent cells. The chemotactically antibiotic solution used is ciprofloxacin, because ciprofloxacin does not kill *E. coli* while can stop the multiplication of *E. coli* by inhibiting the reproduction and repair of the genetic material.⁴⁶ To prepare the antibiotic solution, we dissolve 10 mg ciprofloxacin powder into 1 ml water and use hydrochloric acid to adjust the pH value at 3.5. We dilute it to different concentrations and pour them into reagent cells. After that, the capillary tubes are immersed in the antibiotic solution to study the chemotactical phenomenon. As we infuse the drug from the lower channel, an antibiotic gradient distribution is formed through the whole channels. Bacteria will move toward the upper layer where the drug concentration is low and food is copious. As a result, GFP fluorescence will be reinforced at the top layer which steps up the chemotactic effect. After 4 days, the fluorescence intensity decreases with the increasing of the ciprofloxacin concentration in the reagent cell. Specifically, almost all the *E. coli* bacteria migrate out of the chamber of C1 (800 ng ml^{-1}), C2 (700 ng ml^{-1}), D1 (1200 ng ml^{-1}), D2 (1100 ng ml^{-1}), D3 (1000 ng ml^{-1}), and D4 (900 ng ml^{-1}) as shown in Fig. 5d; a few amount of bacteria move out of the chamber of B1 (400 ng ml^{-1}), B2 (300 ng ml^{-1}), C3 (600 ng ml^{-1}) and C4 (500 ng ml^{-1}); there is no obvious change in the chamber of A1 (no ciprofloxacin), A2 (10 ng ml^{-1}), A3 (20 ng ml^{-1}), A4 (30 ng ml^{-1}), B3 (100 ng ml^{-1}), and B4 (200 ng ml^{-1}). Fig. 6 shows the relationship of bacterial motion *versus* time in chamber C2. It is clearly seen that after 4 days incubating most of the bacteria move out of the chambers upwards to the channels and sample inlets. The drug screening result proves that the wax bonded 3D chip has no adverse factor on antibiotic molecules and culture medium after long term incubation. The chip has good sealing ability which avoids the volatilization of water medium. Bacteria keep alive and move freely inside the system.

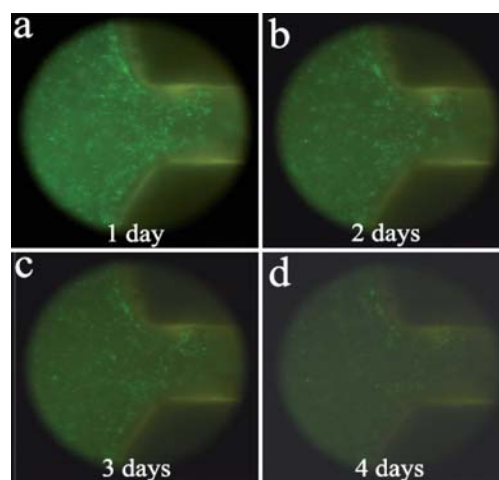


Fig. 6 The *E. coli* bacteria migrate out of chip after (a) 1 day, (b) 2 days, (c) 3 days, and (d) 4 days.

The chip has good optical transparency and could be applied to other cell based drug screening systems in the future.

Conclusions

We report a low-cost and detachable microfluidic chip utilizing easily accessible paper, glass slides or other thin materials as the basic materials along with hot-melt wax as the reversible bonding material. The chip fabrication process is controlled by venting and vacuuming in a hot-water bath. After vacuuming the chamber, the melt wax in the channel is driven out of the chip by negative pressure, while the other wax squeezed between the materials, is retarded by the interfacial absorption so as to play its key role in chip bonding after post-cooling. Laser cutting technology is used to cut through the paper or film to form a channel. The paper or film is then sandwiched between glass sheets or polymer membranes where the wax could form bonding among various materials, such as PMMA, PC, glass sheet, or metal plate. The wax-based chip is detachable in so far as the bonding process is reversible by means of re-melting the wax. We first use the PCR to test the biocompatibility of chip materials with DNA and protein. Subsequently, a microfluidic chip prototype incorporating metal thin layers as electrodes is fabricated. The applicability of the electrodes is tested by subjecting them to HeLa cell electroporation. The influence of voltage on the electroporation efficiency is determined by comparing the cells of bright field phase with the fluorescence phase. With this technology, a 3D microfluidic chip is achievable by one-step. We are able to overlap five layers of different materials together, and vent and vacuumate it in a hot-water bath. To test the sealing ability and durability of the 3D microfluidic chip, GFP recombinant *E. coli* bacteria are cultured in 4 × 4 screening chambers. After 15 days of incubation, the bacteria maintain their fluorescence, and they recover their motility after culturing them again in the tube. Thereby, it is proved that the wax-bonded chip has good sealing ability, durability and effective biocompatibility over long cell culture periods. We added different concentrations of antibiotic ciprofloxacin to the cell reagent to stop the multiplication of *E. coli* and study the chemotaxis of the *E. coli* versus time. Because the 3D chip is transparent and can be applied to drug screening, the screening image indicates that the *E. coli* bacteria could migrate through the channel without being absorbed by the wax or channel wall. The 3D device offers good optical transparency and low background fluorescence, making it applicable to optical detection on-chip.

Acknowledgements

This publication is based on work partially supported by Award No. SA-C0040/UK-C0016, made by King Abdullah University of Science and Technology (KAUST), Hong Kong RGC grants HKUST 603608. The work was also partially supported by the Nanoscience and Nanotechnology Program at HKUST.

Notes and references

- 1 Y. Xia and G. M. Whitesides, *Annu. Rev. Mater. Sci.*, 1998, **28**, 153.
- 2 J. C. McDonald, D. C. Duffy, J. R. Anderson, D. T. Chiu, H. Wu, O. J. A. Schueller and G. M. Whitesides, *Electrophoresis*, 2000, **21**, 27.

- 3 Y. Xia and G. M. Whitesides, *Angew. Chem., Int. Ed.*, 1998, **37**, 550.
- 4 D. Duffy, J. McDonald, O. Schueller and G. M. Whitesides, *Anal. Chem.*, 1998, **70**, 4974.
- 5 X. Zhao, Y. Xia and G. M. Whitesides, *J. Mater. Chem.*, 1997, **7**, 1069.
- 6 R. Mukhopadhyay, *Anal. Chem.*, 2007, **79**, 3248.
- 7 M. W. Toepke and D. J. Beebe, *Lab Chip*, 2006, **6**, 1484.
- 8 J. N. Lee, C. Park and G. M. Whitesides, *Anal. Chem.*, 2003, **75**, 6544.
- 9 Y. S. Heo, L. M. Cabrera, J. W. Song, N. Futai, Y. C. Tung, G. D. Smith and S. Takayama, *Anal. Chem.*, 2007, **79**, 1126.
- 10 J. R. Anderson, D. T. Chiu, R. J. Jackman, O. Cherniavskaya, J. C. McDonald, H. Wu, S. H. Whitesides and G. M. Whitesides, *Anal. Chem.*, 2000, **72**, 3158.
- 11 Y. Luo and R. N. Zare, *Lab Chip*, 2008, **8**, 1688.
- 12 H. S. Chuang and S. Wereley, *J. Micromech. Microeng.*, 2009, **19**, 045010.
- 13 E. Carrilho, A. W. Martinez and G. M. Whitesides, *Anal. Chem.*, 2009, **81**, 7091.
- 14 Y. Lu, W. Shi, L. Jiang, J. Qin and B. Lin, *Electrophoresis*, 2009, **30**, 1497.
- 15 G. V. Kaigala, S. Ho, R. Penterman and C. J. Backhouse, *Lab Chip*, 2007, **7**, 384.
- 16 A. W. Martinez, S. T. Phillips and G. M. Whitesides, *Proc. Natl. Acad. Sci. U. S. A.*, 2008, **105**, 19606.
- 17 X. Li, J. Tian, T. Nguyen and W. Shen, *Anal. Chem.*, 2008, **80**, 9131.
- 18 A. W. Martinez, S. T. Phillips, E. Carrilho, S. W. Thomas, H. Sindi and G. M. Whitesides, *Anal. Chem.*, 2008, **80**, 3699.
- 19 A. W. Martinez, S. T. Phillips, M. J. Butte and G. M. Whitesides, *Angew. Chem., Int. Ed.*, 2007, **46**, 1318.
- 20 S. K. Sia, V. Linder, B. A. Parviz, A. Siegel and G. M. Whitesides, *Angew. Chem., Int. Ed.*, 2004, **43**, 498.
- 21 Y. Lu, W. Shi, J. Qin and B. Lin, *Anal. Chem.*, 2010, **82**, 329.
- 22 M. A. Witek, M. L. Hupert, D. S. Park, K. Fears, M. C. Murphy and S. A. Soper, *Anal. Chem.*, 2008, **80**, 3483.
- 23 J. S. Buch, F. Rosenberger, W. E. Highsmith, C. Kimball, D. L. DeVoe and C. S. Lee, *Lab Chip*, 2005, **5**, 392.
- 24 J. P. Rolland, R. M. V. Dam, D. A. Schorzman, S. R. Quake and J. M. DeSimone, *J. Am. Chem. Soc.*, 2004, **126**, 2322.
- 25 V. I. Ullev, J. Wan, V. Heinrich, P. Landsman, P. E. Bower, B. Xia, B. Millare and G. Jones, *J. Am. Chem. Soc.*, 2006, **128**, 16062.
- 26 S. Metz, R. Holzer and P. Renaud, *Lab Chip*, 2001, **1**, 29.
- 27 D. A. Bartholomeusz, R. W. Boutté and J. D. Andrade, *J. Microelectromech. Syst.*, 2005, **14**, 1364.
- 28 H. Klank, J. P. Kutter and O. Geschke, *Lab Chip*, 2002, **2**, 242.
- 29 H. Liu and H. Gong, *J. Micromech. Microeng.*, 2009, **19**, 037002.
- 30 O. Rötting, W. Röpke, H. Becker and C. Gärtner, *Microsyst. Technol.*, 2002, **8**, 32.
- 31 R. T. Kelly and A. T. Woolley, *Anal. Chem.*, 2003, **75**, 1941.
- 32 P. K. Yuen and V. N. Goral, *Lab Chip*, 2010, **10**, 384.
- 33 H. Wada, H. Sasaki and T. Kamijoh, *Solid-State Electron.*, 1999, **43**, 1655.
- 34 I. A. Choudhury and S. Shirley, *Opt. Laser Technol.*, 2010, **42**, 503.
- 35 M. A. Shoffner, J. Cheng, G. E. Hvichia, L. J. Kricka and P. Wilding, *Nucleic Acids Res.*, 1996, **24**, 375.
- 36 P. Wilding, M. A. Shoffner and L. J. Kricka, *Clin. Chem.*, 1994, **40**, 1815.
- 37 S. Baron, J. Poast, D. Rizzo, E. McFarland and E. Kieff, *J. Immunol. Methods*, 2000, **242**, 115.
- 38 U. Čegovnik and S. Novaković, *Bioelectrochemistry*, 2004, **62**, 73.
- 39 M. Golzio, J. Teissié and M. P. Rols, *Proc. Natl. Acad. Sci. U. S. A.*, 2002, **99**, 1292.
- 40 Y. Huang and B. Rubinsky, *Biomed. Microdevices*, 1999, **2**, 145.
- 41 Y. Huang and B. Rubinsky, *Sens. Actuators, A*, 2001, **89**, 242.
- 42 Y. Huang and B. Rubinsky, *Sens. Actuators, A*, 2003, **104**, 205.
- 43 T. Tsukamoto, N. Hashiguchi, S. M. Janicki, T. Tumber, A. S. Belmont and D. L. Spector, *Nat. Cell Biol.*, 2000, **2**, 871.
- 44 S. Park, P. M. Wolanin, E. A. Yuzbashyan, P. Silberzan, J. B. Stock and R. H. Austin, *Science*, 2003, **301**, 188.
- 45 S. Park, P. M. Wolanin, E. A. Yuzbashyan, H. Lin, N. C. Darnton, P. Silberzan, J. B. Stock and R. H. Austin, *Proc. Natl. Acad. Sci. U. S. A.*, 2003, **100**, 13910.
- 46 R. H. Austin, C.-K. Tung, G. Lambert, D. Liao and X. Gong, *Chem. Soc. Rev.*, 2010, **39**, 1049.